

Thermal Expansion of Copper, Silver, and Gold at Low Temperatures

G. K. White and J. G. Collins

CSIRO Division of Physics, National Standards Laboratory
Sydney, Australia

(Received October 4, 1971)

Improvements have been made in a differential dilatometer using the three-terminal capacitance detector. The dilatometer is of copper and has been calibrated from 1.5–34 K in an extended series of observations using silicon and lithium fluoride as low-expansion reference materials. The expansion of silver and gold samples has been measured relative to the dilatometer, while the calibrations themselves have been used to determine the expansion of copper relative to the reference materials. Analyses of six sets of observations indicate that below 12 K the linear expansion coefficient α of copper is represented by

$$10^{10}\alpha = (2.1_5 \pm 0.1)T + (0.284 \mp 0.005)T^3 + (5 \pm 3) \times 10^{-5}T^5 \text{ K}^{-1}$$

corresponding to respective electronic and lattice Grüneisen parameters $\gamma_e = 0.9_3$ and $\gamma_0 = \gamma_1 = 1.78$. Measurements on oxygen-free silver yield

$$10^{10}\alpha = (1.9 \pm 0.2)T + (1.14 \mp 0.03)T^3 + (2 \pm 2) \times 10^{-4}T^5 \text{ K}^{-1}$$

below 7 K, whence $\gamma_e \simeq 0.9_7$, $\gamma_0 = \gamma_1 = 2.23$. By contrast, silver containing ca. 0.02 at. % oxygen showed a much larger expansion at the lowest temperatures: below 7 K, $10^{10}\alpha \sim 7T + 1.19T^3$. We have not been able to obtain an unambiguous representation for gold, but find a reasonable fit below 7 K to be

$$10^{10}\alpha \simeq (1 \pm 0.5)T + (2.44 \mp 0.05)T^3 - (5 \pm 1) \times 10^{-3}T^5 \text{ K}^{-1}$$

with $\gamma_1 \simeq 2.94$ and $\gamma_e \gtrsim 0.7$ (free-electron value).

1. INTRODUCTION

Carr, McCammon, and White¹ reported measurements from 1.5 to 30 K on high-purity copper which indicated that at temperatures below 10 K the linear expansion coefficient could be represented by

$$10^{10}\alpha = (1.45 \pm 0.15)T + (0.28 \pm 0.01)T^3 \quad (1)$$

The two terms on the right-hand side were identified respectively as electronic e and lattice l in origin and lead to the following values of the Grüneisen parameter :

$$\gamma_e = 0.63 \pm 0.06 \quad \gamma_l = \gamma_0 = 1.72 \pm 0.03$$

This parameter γ is defined by $\gamma = \beta V B_s / C_p$, where β is the volume coefficient of expansion, C_p/V is the specific heat per unit volume, and B_s is the adiabatic bulk modulus.

Carr and Swenson² reported rather similar values for copper in 1964 :

$$10^{10}\alpha = (1.7 \pm 0.5)T + (0.29 \pm 0.02)T^3$$

There followed other measurements, which for $T \lesssim 10$ K gave

$$10^{10}\alpha = (2.78 \pm 0.25)T + (0.310 \pm 0.008)T^3 \quad \text{Shapiro } et \text{ al.}^3$$

$$10^{10}\alpha = (1.55 \pm 0.07)T + (0.275 \pm 0.008)T^3 \quad \text{Kos and Lamarche}^4$$

$$10^{10}\alpha = 1.3 T + 0.27 T^3 \quad \text{Pereira } et \text{ al.}^5$$

$$10^{10}\alpha = (2.32 \pm 0.08)T + (0.325 \pm 0.004)T^3 \quad \text{Graham}^6$$

We conclude that for copper the lattice contribution is known within about 10%, e.g., $10^{10}\alpha_l \simeq (0.30 \pm 0.03)T^3$, corresponding to $\gamma_l = \gamma_0 \simeq 1.9 \pm 0.2$, while the electronic contribution is much more uncertain: $10^{10}\alpha_e \simeq (2 \pm 1)T$.

For silver and gold the situation is even less satisfactory: there are no reported estimates of the electronic terms, but our preliminary data⁷ showed that for silver $\gamma_l = 2.2 \pm 0.1$, while recent data of Kos and Lamarche⁴ give

$$\gamma_l = 2.06 \pm 0.07 (\text{Ag}) \quad \gamma_l = 2.92 (\text{Au})$$

Their results for silver and gold, unlike copper, show a marked variation in $\gamma(T)$ between 9 and 5 K with no sign of γ approaching a low-temperature limiting value. This is rather unexpected and casts some doubt on their experimental accuracy for the following reasons.

The parameter γ_l can be calculated from lattice dynamical models of solids^{7,8}:

$$\gamma_l = \frac{\sum_i \gamma_i C_i / \sum_i C_i}{\gamma_l} \quad (2)$$

where the weighting factor C_i is the contribution of the i th lattice mode, frequency ω_i , to the specific heat, and the mode gamma

$$\gamma_i = -(d \ln \omega_i / d \ln V)_T \quad (3)$$

At high temperatures, i.e., $T >$ the Debye characteristic temperature θ , C_i is equal to Boltzmann's constant k , and $\gamma_i = \gamma_\infty$ is a constant, the simple average of the γ_i . At very low temperatures, $C_i \propto c_i^{-3/2}$, where c_i is the elastic modulus for the i th mode, and $\gamma_i = \gamma_0$ is again constant, albeit different from the high-temperature value.

Barron's model of cubic metals⁸ suggests that γ_0 may be smaller than γ_∞ by 0.2–0.3 and that the major change should occur in the vicinity of $\theta/10$. Barron and others have pointed out that at low temperatures a small minimum may occur in $\gamma(T)$ rather like that occurring in $\theta(T)$ if dispersion in the lattice spectrum gives a heavier statistical weight to those modes with smaller γ_i . Deep minima in $\gamma(T)$ are, in fact, observed in the nonmetallic, diamond-structure solids⁷ with a highly dispersive and low-lying transverse branch of the frequency spectrum in which γ_i decreases sharply with increase in wave number k . We have also seen some evidence of a shallow minimum ($\sim 5\%$) in $\gamma(T)$ in sodium chloride around $T \sim \theta/20$. However, it seems most unlikely that a change as large as those indicated by Kos and Lamarche (20% at 5 K, and increasing) can occur in $\gamma(T)$ for the noble metals, for which anisotropy and dispersive effects are not particularly great.

During the past three years we have been using a new three-terminal capacitance dilatometer for measuring expansion effects in alkali halides, transition metals, alkaline earths, anisotropic materials, and coppers containing impurities. In the course of calibrating the dilatometer we have produced a considerable body of data on the expansion of the copper cell relative to several materials of known thermal expansion, e.g., Si, LiF, and MgO. The calibrations themselves can therefore be used to determine indirectly the expansion coefficient of copper provided that due care is taken to allow for the different size of sample and cell, the nature of the "known" specimen, the presence of bonded surfaces in the cell, etc. (see Sections 2.4 and 2.5). We have also taken sufficient data on samples of silver and gold to be able to report with more confidence the values for the lattice contribution to expansion and hence $\gamma(T)$. There is still considerable uncertainty in the magnitude of the small electronic component.

It is now also possible to compare our data on the noble metals with those obtained by C. A. Swenson and his collaborators⁹ in their extensive series of measurements made with another very sensitive instrument—the differential transformer.

2. EXPERIMENTAL DETAILS

2.1. Cryostat and Capacitance Cell

These are shown schematically in Fig. 1. The modifications to the cryostat described earlier^{1,10} are as follows.

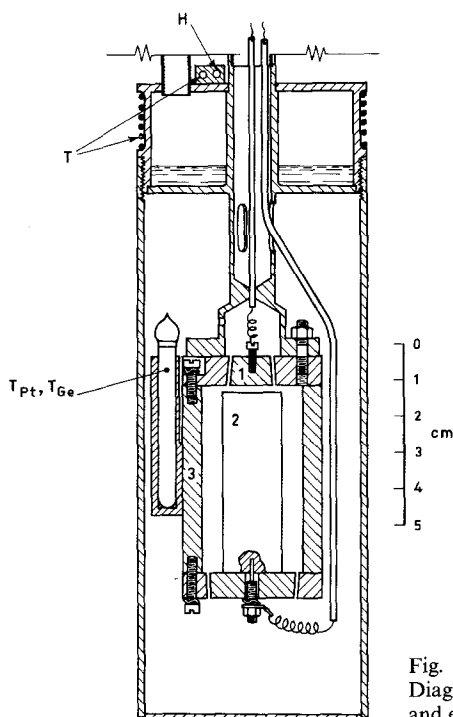


Fig. 1. Three-terminal capacitance dilatometer. Diagram shows only the inner vacuum chamber and expansion cell (OFHC copper).

(i) To aid dismantling and reassembly, the vacuum seal on the outer chamber (not shown in Fig. 1) is now formed by an indium O-ring, and on the inner jacket it is a screw thread greased with silicone. This inner seal remains vacuumtight at room temperature for some hours and is quite satisfactory in operation at low temperatures because the pressure difference across it is very small, the pressures being less than 10^{-6} Torr in the outer vacuum space and of the order of 10^{-2} Torr of helium gas in the inner jacket.

(ii) The platinum and germanium thermometers fit snugly into greased holes in a copper block which is itself in close thermal contact with the cell. The surface of this block has been milled and ground to mate with the outer wall of the cell and is gold plated and greased and held in contact with screws. The thermometers that have been in use in this cell are a Meyers-type platinum thermometer, CT16, used above 11.5 K and a germanium thermometer, Cryocal No. 154, used below 11.5 K. The platinum thermometer has been calibrated here by intercomparison with other platinum thermometers, some of them having been calibrated at the National Bureau of Standards on NBS-55. The germanium thermometer was provided with a commercial calibration but has been checked at NSL against other

germanium thermometers and a constant-volume gas thermometer.¹¹ The electrical leads from these thermometers are thermally anchored around the copper tube which suspends the cell in the inner vacuum space.

(iii) The capacitance cell and the inner chamber including a threaded vacuum jacket are made of OFHC copper which has been stress-relieved before final machining. The top and bottom plates of the cell have central sections approximately 1.25 and 2.5 cm in diameter, respectively, which are insulated from the outer ring by an annular gap of about 0.012 cm, this gap being filled with some Mylar-strip spacers and epoxy resin. The plates and main cylinder for this cell are lapped, gold plated to prevent tarnishing and to assist thermal equilibrium, and then relapped.

(iv) The temperature of the inner chamber is controlled either by pumping a boiling refrigerant (helium or oxygen) into the small chamber or electronically by a temperature controller.¹² This can control temperature to 1 mdeg and is activated by one of the thermometers T (copper resistance or a carbon resistor).

2.2. Measurement Procedure

As discussed previously,¹⁰ the observed capacitance C in pF is related to the gap l by the relation

$$C = k\{r^2/l + [rw/(l + 0.22w)][1 + (w/2r)]\}$$

where r is the radius of the inner plate, and w is the width of the guard gap in centimeters. In our case $2r \approx 1.27$ cm ($\frac{1}{2}$ in.), and $w = 0.012_5$ cm (0.005 in.); since $w \ll r$ and $l \geq w$, this equation reduces to

$$C \approx (k/l)r^2 \times 1.007$$

or, if the expansion of the radius of the copper plate is taken into account,

$$C_{\text{pF}} \approx (k/l)r^2 \times 1.007 \times (1 + 2\Delta r/r) \quad (4)$$

Ignoring this expansion Δr could introduce errors of 1–2%.

When a new sample is mounted, a check measurement of C and T is taken at ca. 20 and 0°C to give $\bar{\alpha}$ (283 K), and generally also at 90, 80, 70, 60, and 55 K before cooling to helium temperatures. Then a series of readings of C (which is often ~ 10 pF and may be read to 10^{-7} pF) and corresponding values of T (to 1 mK) are taken at ca. 35 different temperatures between 1.5 and 30 or 35 K; 4.225 K is the reference or fiducial temperature, and C is checked there frequently to ensure that no apparent drifts or irregular changes in $l_{4.2}$ have occurred. At temperatures near 12 K, both the germanium and Pt thermometers are read and normally found to agree within ca. 5 mK.

We calculate values of l from Eq. (4) and thence the changes Δl relative to 4.225 K. In a calibration run with a specimen such as silicon, corrections are made for the silicon expansion and a table of $\Delta l(T)$ produced by least-squares fitting on a computer. We have found that equations of the form $\Delta l = a + bT^2 + cT^4$ can be used over suitable temperature intervals, e.g., 1.5–9, 9–16, and 16–34 K, with the higher temperature equations adjusted slightly so that values as well as first derivatives are continuous at the junction between ranges. For subsequent experiments on other materials, this table is used to correct the Δl values for the cell's expansion, and then $\bar{\alpha}(T)$ values are calculated from each pair of adjacent values of Δl and T .

2.3. Specimens

The specimens referred to in this paper are as follows (the Si specimens are shown in Fig. 2).

Si 1a: cylinder 5.08 cm long \times 2.2 cm diam; 100 Ω -cm n type from Merck, Sharp, and Dohme, plated with ca. 0.002 cm of nickel (1967–1968), and later (1969) with a layer of evaporated silver.

Si 1b: the same, plus evaporated gold layer.

Si 1c: the same, after cleaning, relapping, electroless nickel plating and coating with final film of gold.

Si 2a: cylinder 4.48 cm long \times 1.9 cm diam with a 0.2-cm hole along central axis and a copper end cap 0.60 cm thick; 100 Ω -cm n -type from du Pont de Nemours.

Si 2b: the same, after being cut into two cylinders, which were ground and lapped to lengths of 2.56 and 1.73 cm. These were mounted together with a copper end piece 0.80 cm long.

Si 2($\frac{1}{2}$): the 2.56-cm portion of Si 2b with a copper end piece 2.52 cm long.

LiF: 5.08 cm long \times 2.2 cm diam, optical quality crystal from Isomet Corp., N.J., ground and coated with an evaporated film of silver.

Cu 2: 5.09 cm long \times 1.9 cm diam, 99.999 + %, Asarco, from American Smelting and Refining Co., N.Y.; their spectroanalysis quoted <1 ppm Fe, Sb, or Cr and <2 ppm As and Te; annealed at 500°C in vacuo after machining.

Cu 3: 5.09 cm long \times 1.9 cm diam, OFHC from Utility Brass and Copper Co., N.Y.; stress-relieved at about 400°C after machining.

Ag 1a: 5.09 cm long \times 2.5 cm diam, as received, "High-Purity Tadanac 99.999%" from Consolidated Mining and Smelting Co. of Canada, obtained in 1961 and not specified as "oxygen-free." Maker's analysis showed ≤ 1 ppm of metallic impurities. Because the expansion seemed to be anomalously high below 15 K (see Section 3.3), a slice was removed by spark erosion and the following tests were done: (i) residual electrical resistance ratio ($RRR =$

$R_{293}/R_{4.2}$) was determined to be ~ 2000 ; (ii) spectroanalysis by Australian Mineral Development Laboratories showed < 2 ppm Fe, < 1 ppm Mn (below the limits of detection); (iii) gas analysis at Defence Standards Laboratory,* Victoria, showed 0.026 at. % oxygen and 0.004 at. % nitrogen; (iv) neutron activation analysis by Gulf General Atomics of California showed 0.011 at. % oxygen.

Ag 1b: the same, after relapping.

Ag 1c: the same, after degassing by pumping for 1 day at 800°C (during which gas evolution began at $\sim 700^\circ\text{C}$) and relapping.

Ag 2: 5.09-cm-long \times 1.6-cm-diam cylinder of 99.999% Tadanac "oxygen-free" from Consolidated Mining and Smelting Co. of Canada, annealed at 500°C for 2 h after machining and then lapped.

Ag 3: 5.09 cm long \times 1.7 cm diam, cast here in graphite from Johnson-Matthey rods ("Specpure" JM 24757) which were degassed at 800°C for some hours before melting.

Au 1: 5.09-cm-long \times 1.9-cm-diam cylinder of "fine" gold ($> 99.9\%$) from Matthey Garrett Ltd. Chemical analysis at Australian Mineral Development Laboratories showed 70 ppm Fe and < 10 ppm Mn.

Au 2: 5.09-cm-long \times 1.6-cm-diam cylinder cast here in graphite (ATJ grade) from Matthey Garrett "refined" gold ($> 99.95\%$).

2.4. Calibration History

A differential cell (as in Fig. 1) is simpler to use than an absolute cell^{1,9} but requires calibration with a material of known expansion. Such materials should be isotropic and have a small expansion coefficient at low temperatures, e.g., MgO, Ge, Si.

In the present cell we have relied chiefly on silicon for which there are now considerable data at low temperatures¹³⁻¹⁵ and also LiF as a check material. Both have fairly high Debye temperatures ($\theta_0 = 650, 740$ K, respectively) and therefore a small expansion at low temperatures. From experiments¹⁶ on alkali halides the expansion behavior of lithium fluoride is known to be regular at moderately low temperatures; it has an expansion coefficient which is proportional to the heat capacity, with the proportionality constant given by the limiting value of the Grüneisen parameter γ_0 . Both expansion data and pressure derivatives of the elastic constants indicate that γ_0 lies between 1.7 and 1.8.

Errors arising from the cell calibration in terms of these solids are discussed in Section 2.4. Some details of the calibrations are necessary for an understanding of the different sets of copper expansion values and are given below.

*This test was kindly performed by Mr. A. Lench at Maribyrnong.

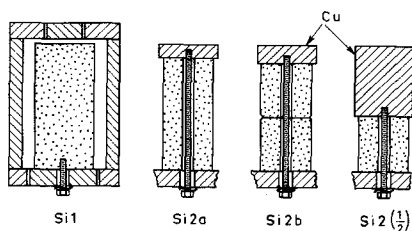


Fig. 2. The silicon cylinders shown with either conducting layers of nickel and silver (or gold) or a solid copper end piece.

(i) *December 1967/January 1968*. Initial calibration runs in the new cell were done with Si 1a, a cylinder shown in Fig. 2 which was plated by an electroless nickel process to provide continuous electrical surface at low temperatures, and with Cu 2 (Asarco copper). These were followed by measurements on a number of substances—Pd, Rh, and Ir,¹⁷ some alkali halides including NaCl, KCl, and RbBr, and low-expansion materials, namely, Cer-Vit and Corning U.L.E. silica.¹⁸

(ii) *January/February 1969*. Recalibration runs with Si 1a and Si 2a showed that sensitivity was being limited by electrical instability, caused by intermittent breakdown across the guard-ring gap in the upper plate. This gap had been less than 0.007 cm. A new upper plate was made with a gap of 0.012 cm, the cell reassembled, and calibrations started afresh.

(iii) *March/May 1969*. Two calibration runs were done with Si 1a (having an evaporated layer of silver on top of the nickel plate to ensure a continuous surface) and LiF, and one with Cu 2. These yielded two sets of data for the copper relative to Si 1 and to LiF which are collectively called Series I.

These were followed by preparation of a calibration table and measurements on CaF₂ and BaF₂; further work on Pd, Rh, and Ir;¹⁷ Ag 2, Ag 1b, and Au 2 (reported in this paper); the anisotropic metals As and Sb;¹⁹ and the alkali halides RbCl, NaF, NaBr, and CsF.¹⁹

(iv) *June/July 1970*. After remeasuring Cu 2 and Cu 3, a second series (Series II) of calibration runs was carried out.*

Si 1b: after evaporating a fresh layer of gold on the surface.

Si 2a: 4.48 cm long with a 0.60-cm copper end piece.

Si 1c: after cleaning, replating with nickel, and freshly evaporating a surface of gold.

Si 2b: after cutting Si 2 into two pieces, 2.56 cm and 1.73 cm long (total 4.29 cm), which were lapped and mounted together with a copper end piece 0.80 cm long (see Fig. 2).

*This was stimulated by correspondence with C. A. Swenson showing that measurements at Iowa State University⁹ were giving rather different values for both copper and silver below 15 K.

Si 2($\frac{1}{2}$): one of the previous two pieces 2.56 cm long, with an end piece of copper 2.52 cm long.

Finally, two copper cylinders (OFHC) 2.56 and 2.53 cm long were put together just as the two cylinders of Si 2b had been, to see if measurements agreed with those for one single copper cylinder Cu 3, which they did.

2.5. Errors in Calibration with Si and LiF: 1.5–34 K

Consider first the systematic errors which may arise from uncertainties in $\alpha(T)$ for Si or LiF. In the case of Si their importance may be judged from Table I in which the expansivities of the silicon sample and copper cell are compared up to 34 K. Below 15 K we have used data for silicon from Sparks and Swenson,¹⁴ although these lead to a value of $\gamma_0 \approx 0.44$, appreciably higher than the value of $\gamma_0^{el} = 0.24$ calculated from elastic data. If indeed these data overestimate α by a corresponding amount then we find from Table I that the cell calibration values are in error by ca. 1% (too large). From 20–30 K we have preferred the data of Carr *et al.*,¹³ which agree with those of Ibach.¹⁵ If in this region Sparks and Swenson's values are better,

TABLE I
Expansivity $\Delta l/l$ of Silicon Compared with the Copper Cell
(August 1970)

T, K	$10^8 \Delta l/l$, silicon	$10^8 \Delta l/l$, Cu cell
2	-0.007	-0.301
3	-0.005	-0.225
4.225	0	0
5	+0.006	0.261
6	+0.020	0.809
7	+0.045	1.68
8	+0.083	2.99
10	+0.21	7.46
12	+0.45	15.6
14	+0.83	29.4
16	+1.4	50.9
18	+1.8	82.8
20	+1.4	129.3
22	-0.2	194.0
24	-2.2	281.1
26	-6.3	394.9
28	-12.5	540.2
30	-21.5	722.1
32	-40.5	946.3
34	-57	1219

the silicon corrections should be decreased by $\sim 20\%$, and the present cell calibration would be ca. $\frac{1}{2}\%$ too small.

Another possible source of error arises when using semiconductors like silicon to form a capacitance plate for measuring expansion; Carr *et al.*¹³ traced an unduly large change in apparent length to "pinholes in the silver (conductive coating) which had been evaporated . . . (onto the silicon) . . . to define the electrical capacitance surface and to connect it electrically to the lead to the capacitance bridge . . . The resistance of germanium and silicon increases rapidly below 20 K and exposed areas of semiconductor surface at the pinholes cause a spuriously large change in capacitance (and apparent sample length) . . ." To overcome this possibility we have done two things. Firstly Si 1 was coated with nearly 1 mil of nickel*; later, evaporated coats of silver or gold were added to see whether any change resulted in the expansion behavior at low temperatures. Secondly, Si 2 (which had been a smaller cylinder used before in our absolute cell) was fitted with a copper end cap to form the electrical surface (see Fig. 2). Small differences which were observed in the Si calibration runs cannot be attributed to pinhole effects.

Lithium fluoride, used in Series I, is an alkali halide for which γ is sensibly constant. Earlier measurements¹⁶ of thermal expansion indicated that $\gamma_0 = 1.7$ (compare $\gamma_\infty = 1.66$), whereas calculations based on elastic constants and their pressure derivatives indicated that $\gamma_0 \approx 1.8$. Using a compromise value, $\gamma = 1.75$, we deduce from specific heat behavior and compressibility that

$$\alpha = 8.0 \times 10^{-12} T^3 + 1.3 \times 10^{-15} T^5 \quad T < 30 \text{ K}$$

and obtain correction values of $\Delta l/l$ which are about 30% of the corresponding expansion values for copper. If γ were 1.8 rather than 1.75 our corrections would be in error by about 3% and cause a corresponding error of 1% in the calibration. A comparison of the deviations of individual calibration points obtained in March/May 1969 (Series I) from the computed mean indicated that LiF-based data are up to 1% higher than Si 1-based data. These deviations include random errors and have rms values of 0.06 Å (1.5–9 K), 0.16 Å (9–15 K), and 6 Å (15–30 K), the maximum departures from the mean reaching about 0.1 Å at 9 K (0.5%), 0.3 Å at 15 K (0.2%), and 10 Å at 30 K (0.3%).

The 1970 calibration table (June/July 1970 or Series II) was prepared from four runs with Si 1 and Si 2. These differed among themselves more than did the two runs in Series I, the rms deviation being 0.19 Å (2–9 K), 1.3 Å (9–17 K), and 10 Å (17–35 K), the maximum departures from the computed mean reaching ca. 0.4 Å at 9 K (2%), 2 Å at 15 K (1%), and 20 Å

*This was done thanks to the kind help of Mr. Bill Eade at the Research Laboratory of the Amalgamated Wireless Valve Co., Rydalmere, NSW.

at 34 K (0.3%). Two other runs were done, a repeat of Si 2b and Si 2($\frac{1}{2}$). Results from these composite samples, which were not used in the computed table, also showed departures of 1–2% from previous runs. In particular, the 2.5 cm long Si 2($\frac{1}{2}$) showed large departures between 15 and 30 K (amounting to 3–4%) but below 12 K agreed closely with the mean. The reasons for discrepancies between sets of observations are puzzling. We conclude that at different times the surfaces of Cu and Si, for example, mate differently, so that although thermal cycling from 4 \rightarrow 20 \rightarrow 4 K or 4 \rightarrow 30 \rightarrow 4 K does not show significant hysteresis (\nrightarrow 0.1%), elastic strains occur at the mating surfaces and produce different behaviors at different times.

Apparent systematic differences between the 1969 and 1970 calibrations call for comment; the later series were ca. 3% higher below 10 K, 4% higher from 10–17 K, and fell to 2% higher at 35 K. This we attribute to aging effects in the cell, e.g., in epoxy resins, etc., because copper specimens measured during each of these two periods showed analogous differences. The absolute expansion coefficients for copper, when corrected for cell calibration, showed little difference between the 1969 and 1970 series.

A further insurance against serious systematic errors has come from measurements made in 1970 (as yet unpublished) on three materials, each of fairly small expansion: BaF₂, CaF₂, and NaF. A significant error of, say, 3% in calibration would show up as a large error (\sim 10%) in their α or γ at low temperatures. In fact, γ_0 determined from expansion agrees with γ_0^{el} within combined limits of experimental uncertainty of ca. 5%: for BaF₂, $\gamma_0 = 0.26 \pm 0.03$, $\gamma_0^{el} = 0.26$; for CaF₂, $\gamma_0 = 1.00 \pm 0.07$, $\gamma_0^{el} = 1.0$ –1.1; and for NaF, $\gamma_0 = 0.94 \pm 0.05$, $\gamma_0^{el} = 1.0$.

2.6. Errors in Calibration Using Copper as a Reference Material: 0–20° C and 54–90 K

The sensitivity of the capacitance technique is needed most at low temperatures where coefficients are small, but many measurements have been made also at higher temperatures, conveniently obtained with liquid oxygen or ice. If required, the electronic temperature-control system can maintain temperatures outside these ranges.

For calibration purposes we measured samples of copper in the cell and used existing reference data on copper to give an effective expansion coefficient for the cell.

0–20°C. Samples of both Asarco copper (Cu 2) and OFHC (Cu 3) in the cell (itself OFHC) have shown that from 0–20°C

$$\alpha_{Cu} - \alpha_{cell} = (0.03 \pm 0.01) \times 10^{-6} \text{ K}^{-1}$$

Previously we have used $\alpha_{Cu} \approx 16.6 \times 10^{-6}$ at 283 K based chiefly on the data of Rubin *et al.*²⁰ However, new data from both NBS²¹ and NRC²¹

on copper agree very closely down to 90 K and we prefer to use their value of $\alpha_{\text{Cu}} = 16.43 \times 10^{-6} \text{ K}^{-1}$ at 283 K, whence $\bar{\alpha}_{\text{cell}} = 16.40 \times 10^{-6}$. This smaller value is supported by measurements made here on vitreous silica. We obtain $\alpha = 0.46 \times 10^{-6} \text{ K}^{-1}$ for Spectrosil ("fictive" temperature $T_f = 1000^\circ\text{C}$) and $\alpha = 0.37 \times 10^{-6} \text{ K}^{-1}$ for Vitreosil ($T_f = 1400^\circ\text{C}$) in satisfactory agreement with earlier values²² $0.48 \times 10^{-6} \text{ K}^{-1}$ ($T_f = 1050^\circ\text{C}$) and $0.42 \times 10^{-6} \text{ K}^{-1}$ ($T_f = 1100^\circ\text{C}$), respectively, when differences in fictive temperature, and hence density, are considered. We also obtain $10^6\alpha = 2.40 \text{ K}^{-1}$ (283 K) for Si compared with values of 2.47,¹³ 2.40,¹⁵ 2.53,²³ and 2.3 K^{-1} .²⁴

It has been suggested that significant differences sometimes reported for copper arise from minor strains, impurity differences, etc. Our measurements on Asarco copper, OFHC copper, free-machining and touch-pitch copper, and also copper which had been deformed 70%, all contradict this.²⁵ They show differences of less than $0.02 \times 10^{-6} \text{ K}^{-1}$ in $\alpha(283)$ or 0.2%. Even alloys of Cu + 0.2 at. % Fe and Cu + 0.2 at. % Mn differed by only $+0.02 \times 10^{-6}$ and $+0.07 \times 10^{-6} \text{ K}^{-1}$, respectively, from pure copper in the range 0–20°C.

54–90 K. In this temperature range we have measured various copper specimens in the cell, including Asarco, OFHC, deformed and annealed samples,* and Cu + 0.2 at. % Fe. In no instance was there any significant difference ($>0.01 \times 10^{-6} \text{ K}^{-1}$) in the expansion between the cell and the sample. (Note, however, that serious differences *do* arise in the region below 20 or 30 K where magnetic impurities have a marked effect.)

As reference data for copper in this region we have used the following values, smoothed from those of Rubin *et al.*²⁰: $10^6\alpha = 8.94$ (85 K), 7.69 (75 K), 6.26 (65 K), 5.17 (58 K), and 5.01 K^{-1} (57 K). With these our measurements on Si 1 give the following values for silicon: $10^6\alpha = 0.50$ (85 K), 0.48 (75 K), 0.45 (65 K), and 0.38 K^{-1} (58 K), which agree well with corresponding values of $10^6\alpha = 0.48, 0.50, 0.46,$ and 0.37 K^{-1} , respectively, from Carr *et al.*¹³ Hahn²¹ has given α -values for Standard Reference Copper #736 which are ca. $0.1 \times 10^{-6} \text{ K}^{-1}$ smaller in this range, but sufficient doubt exists²⁶ for us to prefer the older values of Rubin *et al.*

2.7. Accuracy of Results: Summary

0–20°C and 54–90 K. Random errors in α are unlikely to exceed $0.02 \times 10^{-6} \text{ K}^{-1}$; systematic errors arising from calibration reference data are probably similar but *could* conceivably be as high as $0.1 \times 10^{-6} \text{ K}^{-1}$.

1.5–34 K. From the differences between calibrating runs, from repro-

*These were examined by Dr. J. S. Rogers in 1965, in collaboration with the CSIRO Division of Tribophysics.

ducibility, and from uncertainties in the behavior of the reference materials such as Si which were mentioned above, we conclude that errors in measurement of length change should be less than 20 Å at 34 K (0.3%), 2 Å at 15 K (1%), 0.2 Å at 9 K (1%), and 0.04 Å at liquid-helium temperatures.

Additional errors in α can arise from the limits of readings of thermometers or errors in temperature scale, e.g., when $\Delta T \sim 0.5$ K, a possible error in ΔT of 5 mK will lead to a 1% error in α . We conclude that errors in α from all sources should be less than $1 \times 10^{-8} \text{ K}^{-1}$ at 34 K (corresponding to $\sim 1\%$ for copper), $0.1 \times 10^{-8} \text{ K}^{-1}$ at 15 K, and $0.03 \times 10^{-8} \text{ K}^{-1}$ at 9 K. At helium temperatures, errors will be at least $0.01 \times 10^{-8} \text{ K}^{-1}$ due to the limits of sensitivity in reading Δl .

3. RESULTS

3.1. Method of Analysis

At sufficiently low temperatures, say $T \lesssim \theta/25$, both the specific heat C_v and the coefficient of thermal expansion α can be expressed as polynomials in odd powers of temperature²⁷:

$$C_v = aT + bT^3 + cT^5 + \dots \quad (5a)$$

$$= aT + b'(T)T^3 \quad (5b)$$

and

$$\alpha = AT + BT^3 + CT^5 + \dots \quad (6)$$

Here, $b \propto [\theta_0(V)]^{-3}$, $b' \propto [\theta(V, T)]^{-3}$, and $B \propto (-d \ln \theta_0/d \ln V)_T$, where $\theta_0(V)$ is the Debye temperature at $T = 0$ and $\theta(V, T)$ is the Debye temperature corresponding to the measured specific heat at T . The linear terms are attributed to conduction electrons, the cubic terms to the lattice vibrations in the long-wavelength limit (the Debye continuum region), and higher order terms to dispersion in the lattice spectrum and to anharmonicity. The alternative equation (5b) for C_v restricts the series to a Debye-type expression, allowing b' and hence θ to be temperature dependent and so implicitly including dispersion as a departure of $\theta(T)$ from θ_0 . This representation of C_v is a useful guide to the analysis of $\alpha(T)$.

Low-temperature expansion measurements may be analyzed in two ways, each based on Eq. (6). The usual approach, which we adopt in this paper, is to plot α/T against T^2 , obtain the electronic coefficient A from the intercept at $T = 0$, the lattice coefficient B from the linear slope of the plot near $T = 0$, and the coefficient C from the *initial* deviation of the slope from a straight line as T increases. Care must be taken to weight appropriately the very lowest points, $T \lesssim 4$ K, which contain increasingly large experimental uncertainties but which are most important in determining A and B . Care

must also be taken above $\theta/50$ – $\theta/40$ to detect the onset of dispersive effects. Here the variation of $\theta(T)$ is a useful index: we have arbitrarily assumed that a variation of about 1 K in $\theta(T)$ from θ_0 indicates the end of the Debye continuum region.

The alternative approach (cf. Ref. 27), used by McLean *et al.*⁹ in the following paper, is to plot $(\alpha - AT)/T^3$ against T^2 . The electronic coefficient A is chosen to give linearity to the distribution as $T \rightarrow 0$; B is given by the intercept at $T = 0$ and C by the initial linear slope. An incorrect choice of A produces a T^{-2} flare in the plot as $T \rightarrow 0$; the same effect magnifies greatly the representation of experimental uncertainties in the lowest temperature data. Care must be taken in this case to ensure that the slope and hence the important intercept B is determined by the *initial* departure of the data from Debye behavior in the region $\theta/50$ – $\theta/30$ and not by a pseudo- T^5 region which can occur above $\theta/30$ in a similar way to the pseudo- T^3 region which has confused some specific heat analyses in the past. Here again the behavior of $\theta(T)$ is an important guide: our criterion is that only measurements taken up to some degrees below the point of inflexion in the $\theta(T)$ vs. T curve (about $\theta/20$ for Cu and Ag) should be used to estimate C . Near the point of inflexion the specific heat can no longer be represented as a simple power series in T (cf. Blackman²⁸), and use of the simple polynomial form to too high a temperature can lead to an incorrect analysis.

We fit our results to the equation $\alpha/T = A + BT^2 + CT^4$, both graphically and using a computer or desk calculator. The coefficients quoted for each metal were obtained by machine fitting, using the following procedure. Starting from the lowest temperatures we successively fit a straight line to the first 3, 4, 5, . . . , n datum points. We use a least-squares criterion and seek values of A and B that stabilize the fit in the sense that addition of each further point does not alter A or B significantly. We cut off the calculation at ca. $\theta/30$, by which temperature $\theta(T)$ has changed by several degrees from θ_0 , and the values of A and B are varying steadily. This cumulative-points procedure is illustrated for copper in Fig. 3 using data from all six runs and fitting $\alpha/T = A + BT^2$ only: note that each point on the plot indicates the fit to *all* data up to that temperature.

The analysis was repeated with the lowest—and hence least certain—points dropped, and for individual runs as well as for the aggregated data. The values chosen for A and B were an average from all such fits, and the errors quoted for the coefficients in the following sections are the systematic differences between fits (i.e., runs) which, although small, tended to be greater than the random experimental uncertainties.

The coefficient C was estimated by plotting $(\alpha - AT - BT^3)/T^5$ against T^2 for all measurements up to the point of inflexion in $\theta(T)$ and choosing an average value of C from that part of the plot ($\sim \theta/50$ – $\theta/30$) running parallel

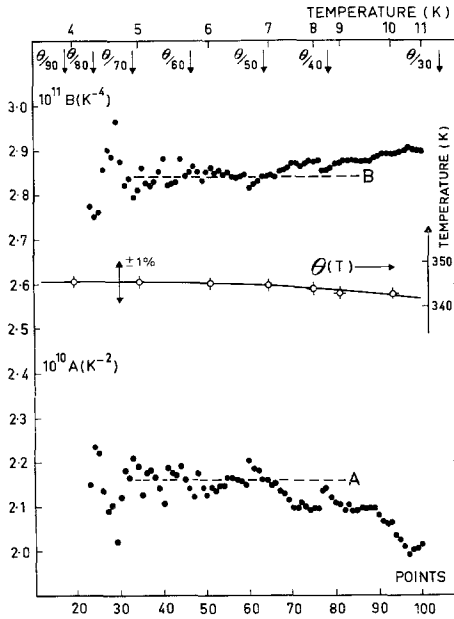


Fig. 3. Coefficients A and B obtained from cumulative-points fits to $\alpha/T = A + BT^2$ for copper for the first 23–100 datum points in Table III. The variation of $\theta(T)$ with T shows a departure from θ_0 from about $\theta_0/50$.

to the T^2 axis. This region is well defined because the distribution departs quite suddenly from the T^2 axis between $\theta/30$ and $\theta/25$. There is a large scatter in the points, which is emphasized by the T^{-5} weighting, and there is a large relative uncertainty in the value chosen for C .

As a final check on the self-consistency of the analysis, the data were plotted as $(\alpha - AT)/T^3$ against T^2 using the value already chosen for A . A satisfactory visual fit was found in each case.

Electronic and lattice Grüneisen ratios, γ_e and γ_0 , respectively, were calculated for each metal in the low-temperature limit using the fitted polynomial for α and the physical data given in Table VI. Individual values for γ_l were calculated for each datum point and these were extrapolated to $T = 0$ as a cross check on γ_0 .

The results for each individual metal are discussed below.

3.2. Copper

Expansion values for copper were derived from the six sets of calibration readings (Table II) in which Si 1, Si 2, or LiF specimens were in the cell.

TABLE II
 Linear Coefficient of Thermal Expansion of Copper: α in units of 10^{-8} K^{-1}

Series I (1969)				Series II (1970)							
Si 1a		LiF		Si 1b		Si 1c		Si 2a		Si 2b	
T	α	T	α	T	α	T	α	T	α	T	α
2.714	0.12 ₅	2.696	0.13 ₅	2.466	0.10 ₅	2.567	0.10 ₅	2.478	0.10	2.444	0.09 ₅
—	—	—	—	3.091	0.14	2.978	0.11	3.110	0.13	3.065	0.13
3.549	0.20 ₅	3.450	0.20 ₅	3.649	0.23	3.387	0.18	3.659	0.21	3.629	0.23
4.060	0.26	3.987	0.25	4.065	0.28	3.898	0.25	4.069	0.26	4.060	0.30
4.440	0.34	4.429	0.36	4.418	0.34	4.411	0.33	4.410	0.35	4.425	0.37
4.871	0.44	4.730	0.43 ₅	4.827	0.43	4.823	0.40	4.815	0.39	4.828	0.40
5.289	0.56	5.278	0.55	5.250	0.53	5.249	0.52	5.248	0.50	5.247	0.55
5.672	0.66	5.654	0.66	5.623	0.63	5.626	0.63	5.630	0.61	5.621	0.58
6.033	0.73	5.998	0.76	5.966	0.75	5.969	0.72	5.974	0.70	5.993	0.78
6.466	0.92	6.386	0.87	6.350	0.88	6.354	0.87	6.350	0.85	6.374	0.85
6.931	1.10	6.893	1.11	6.767	1.05	6.771	1.03	6.762	0.95	6.762	1.04
7.376	1.33	7.559	1.43	7.226	1.26	7.228	1.24	7.226	1.22	7.221	1.24
7.914	1.58	—	—	7.781	1.54	7.780	1.53	7.780	1.49	7.772	1.51
8.553	1.99	8.356	1.85	8.422	1.93	8.426	1.91	8.415	1.87	8.410	1.81
9.246	2.47	9.164	2.38	9.109	2.40	9.119	2.37	9.098	2.32	9.093	2.38
9.988	3.07	9.919	3.03	9.829	2.98	9.834	2.99	9.811	2.93	9.806	2.91
10.760	3.81	10.700	3.70	10.660	3.82	10.659	3.79	10.642	3.74	10.639	3.78

TABLE II—continued

Series I (1969)				Series II (1970)							
Si 1a		LiF		Si 1b		Si 1c		Si 2a		Si 2b	
T	α	T	α	T	α	T	α	T	α	T	α
11.786	4.97	11.769	4.97	11.676	4.90	11.689	4.92	11.675	4.82	11.680	4.85
13.076	6.99	13.052	6.89	12.837	6.68	12.874	6.69	12.845	6.61	12.853	6.68
14.335	9.20	14.278	9.08	14.028	8.80	14.068	8.83	14.036	8.71	14.051	8.73
15.576	12.01	15.511	11.73	15.225	11.31	15.269	11.41	15.230	11.25	15.244	11.35
16.974	15.58	16.895	15.53	16.551	14.77	16.605	14.86	16.560	14.68	16.588	14.80
18.575	21.07	18.478	20.81	18.079	19.50	18.137	19.72	18.088	19.48	18.127	19.71
20.225	27.63	20.135	27.56	19.744	25.96	19.738	25.82	19.676	25.89	19.719	26.00
21.767	35.24	21.831	36.15	21.424	33.93	21.362	33.68	21.345	33.47	21.357	33.79
23.558	46.08	23.706	47.58	23.021	43.20	23.027	43.17	23.006	43.26	22.988	43.40
25.265	57.1	25.611	61.2	24.706	54.4	24.748	54.8	24.705	54.7	24.638	54.4
26.684	70.3	—	—	26.476	68.3	26.478	68.4	26.488	68.7	26.418	68.9
28.159	83.2	27.308	75.4	28.020	81.5	28.034	82.3	28.026	82.2	27.949	82.4
29.606	97.1	28.751	88.5	29.220	93.4	29.307	94.9	29.228	93.8	29.170	93.7
—	—	—	—	30.255	103.3	—	—	30.324	105.1	—	—
—	—	—	—	31.428	116.7	—	—	31.523	117.8	—	—
—	—	—	—	32.669	129.2	—	—	32.785	132.6	—	—
—	—	—	—	33.904	148.0	—	—	33.988	147.5	—	—

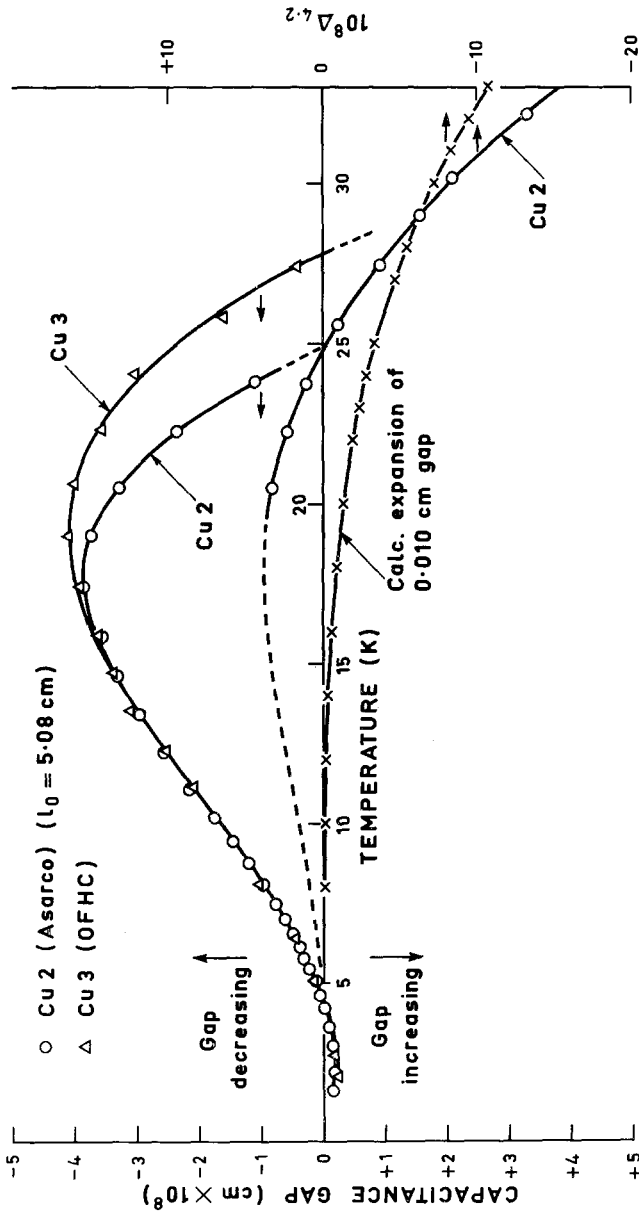


Fig. 4. Small changes observed in capacitance gap when a copper cylinder is in the copper cell. Note difference in scale by factor of four between left and right ordinates.

The readings were first corrected for the small expansion of the Si or LiF and then for the small differences observed when Cu 2 (Asarco) was placed in the cell as a specimen.

Differences between the copper cell and a copper cylinder observed during the Series II calibrations are shown in Fig. 4. In warming from 4.2 to 15 K the gap change is about -4 \AA compared with a total expansion of ca. 190 \AA , and by 30 K it is $+8 \text{ \AA}$ compared with 3600 \AA . Part of this positive change (increase in gap) which is noticeable above 15 K arises from the difference in length, say 0.010 cm , of specimen and frame. The negative change (decrease in gap) predominates below 15 K and arises presumably from the effect of the epoxy resin in the guard gap.

Values for α , determined from neighboring pairs of expansion measurements, are given in Table II and illustrated graphically for the temperature range 15–20 K in Fig. 5. Above 10 K differences between runs are less than 2%; below 10 K accuracy is limited by the resolution of readings, ca. $0.02 \times 10^{-8} \text{ K}^{-1}$ in terms of α , which amounts to $\sim 2\%$ at 7 K and $\sim 5\%$ at 5 K.

Figure 6 shows values of α/T plotted against T^2 for temperatures up to $\theta/40$. Below 12 K computer analysis gives as the equation of best fit

$$10^{10}\alpha \approx (2.1_5 \pm 0.1)T + (0.284 \mp 0.005)T^3 + (5 \pm 3) \times 10^{-5}T^5$$

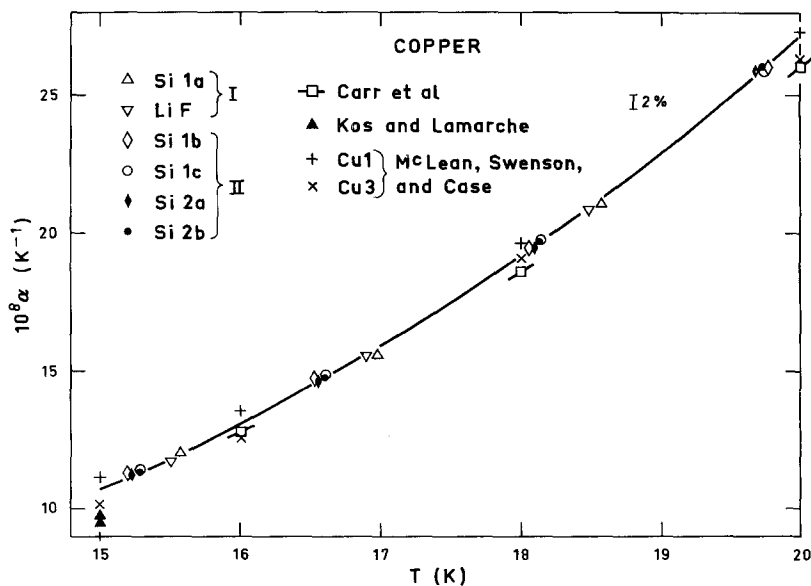


Fig. 5. Linear coefficient of thermal expansion of copper; section from 15–20 K illustrates the agreement with other measurements.^{1,4,9}

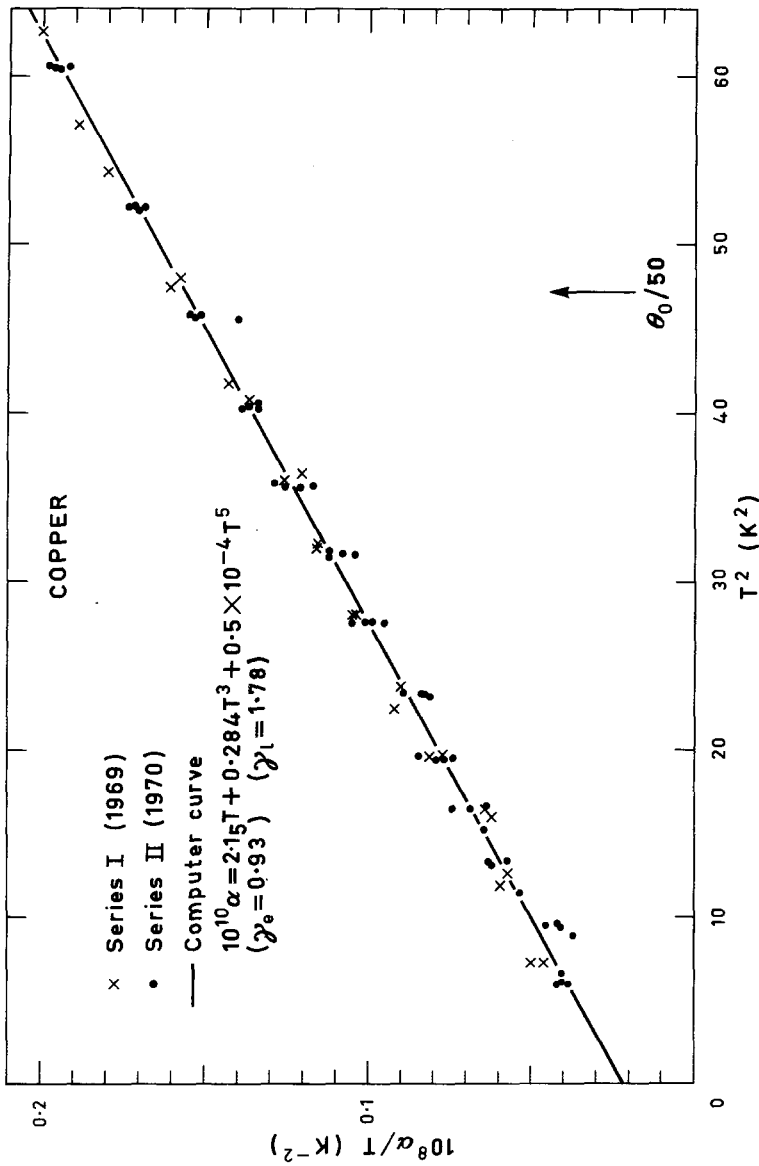


Fig. 6. Values of α/T vs. T^2 for copper ($\theta_0 = 344.5$ K) together with computer-fitted polynomial.

from which we calculate Grüneisen parameters

$$\gamma_e \approx 0.93 \pm 0.04 \quad \gamma_l = \gamma_0 \approx 1.78 \mp 0.03$$

Table V contains smoothed values of the total expansion coefficient α , the lattice component α_l , and γ_l at selected temperatures from 2 K to room temperature. The figures have been obtained from the fitted equation at low temperatures and from a large-scale graph of the data at higher temperatures. Clearly, at temperatures below 20 K, γ_l is close to the limiting value γ_0 and shows no significant variation until $T \sim \theta/10$ (see Fig. 11) when it increases steadily and approaches the high-temperature value $\gamma_\infty \approx 2.0$.

TABLE III
Linear Expansion Coefficient α (Units of 10^{-8} K^{-1}) for Silver

Oxygen-free									
Ag 1b		Ag 2		Ag 3		Ag 1c (8 Oct.)		Ag 1c (12 Oct.)	
<i>T</i>	α	<i>T</i>	α	<i>T</i>	α	<i>T</i>	α	<i>T</i>	α
2.383	0.31	2.428	0.21	2.473	0.22	—	—	2.290	0.14
3.000	0.53	3.051	0.39	3.085	0.40	—	—	3.013	0.34
3.611	0.82	3.629	0.62	3.630	0.61	—	—	3.586	0.57
4.035	1.09	4.055	0.88	4.059	0.82	—	—	4.043	0.79
4.417	1.31	4.414	1.07	4.419	1.05	4.406	1.12	4.435	1.03
4.834	1.78	4.831	1.41	4.816	1.32	4.822	1.40	4.849	1.34
5.257	2.14	5.254	1.78	5.237	1.69	5.250	1.81	5.251	1.69
5.633	2.56	5.628	2.19	5.616	2.08	5.625	2.17	5.625	2.08
5.975	2.99	5.978	2.54	5.964	2.49	5.966	2.56	5.973	2.49
6.373	3.61	6.370	3.15	6.354	2.99	6.354	3.05	6.361	2.98
6.807	4.28	6.790	3.84	6.775	3.58	6.773	3.73	6.778	3.60
7.268	5.14	7.251	4.55	7.235	4.40	7.229	4.52	7.239	4.38
7.824	6.32	7.810	5.76	7.792	5.48	7.785	5.60	7.793	5.47
8.467	7.97	8.451	7.30	8.434	6.94	8.428	7.15	—	—
9.158	9.88	9.135	9.24	9.124	8.83	9.115	9.01	—	—
9.884	12.25	9.857	11.64	9.841	11.16	9.834	11.29	—	—
10.705	15.71	10.676	15.04	10.649	14.48	10.660	14.54	—	—
11.711	20.59	11.691	19.93	11.675	19.35	11.686	19.53	—	—
12.884	28.20	12.868	27.68	12.860	26.74	12.869	26.94	—	—
14.092	37.57	14.069	36.96	14.061	35.94	14.080	36.15	—	—
15.290	48.73	15.268	48.12	15.256	46.82	15.294	47.28	—	—
16.630	63.81	16.657	63.92	16.587	61.79	16.662	62.46	—	—
18.178	84.45	18.248	85.60	18.114	81.94	18.205	82.76	—	—
19.762	108.3	19.846	110.9	19.761	107.0	19.794	107.3	—	—
21.387	136.9	21.477	140.3	21.443	136.6	21.425	136.2	—	—
23.108	169.8	23.112	172.2	23.053	167.6	23.043	168.0	—	—
24.881	207.2	—	—	24.722	203.2	—	—	—	—
26.557	244.3	—	—	26.499	242.1	26.984	253.9	—	—
28.187	283.5	—	—	28.162	281.3	—	—	—	—
29.603	315.3	—	—	—	—	—	—	—	—
—	—	—	—	—	—	30.482	339.2	—	—
—	—	—	—	—	—	31.471	363.5	—	—
—	—	—	—	—	—	32.704	395.2	—	—

3.3. Silver

Results are listed in Table III for three "oxygen-free" samples: Ag 2 (Tadanac "oxygen-free"), Ag 3 (cast here from degassed Johnson-Matthey silver) and Ag 1c (Ag 1 after degassing). These agree sufficiently among themselves (Figs. 7 and 8) and with data sent to us by Swenson⁹ to be considered representative of pure silver.

In addition we include results Ag 1b which are measurements taken in 1970 on sample Ag 1 in the "as-received" condition. These are much larger than measurements on all other samples of silver at temperatures below 10 K and are clearly anomalous. After degassing the sample at 800°C to remove oxygen (see Section 2.3), the expansion results (Ag 1c) agreed with those of Ag 2 and Ag 3 and with those of McLean *et al.*⁹ Results Ag 1b are included as an example of the effect of oxygen impurity on the low-temperature expansion of silver, but are not considered any further. (An earlier, less accurate set, Ag 1a, taken on this sample agrees well with Ag 1b, but is not of sufficient importance to be listed here.)

The computer analyses of runs Ag 2, Ag 3, Ag 1c (8 Oct. 1970), and Ag 1c (12 Oct. 1970) give an equation of best fit below 9.5 K as

$$10^{10}\alpha \simeq (1.9 \pm 0.2)T + (1.14 \mp 0.03)T^3 + (2 \pm 2) \times 10^{-4}T^5 \text{ K}^{-1}$$

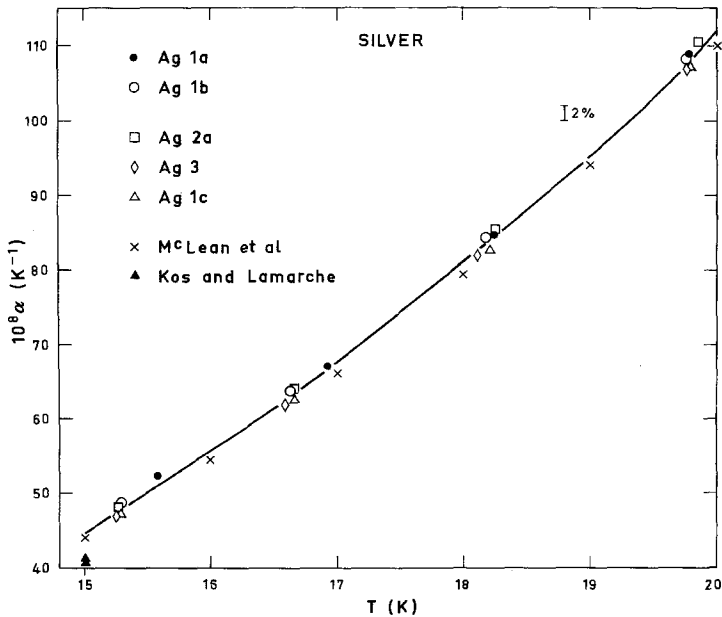


Fig. 7. Linear expansion coefficient of silver, 15–20 K.

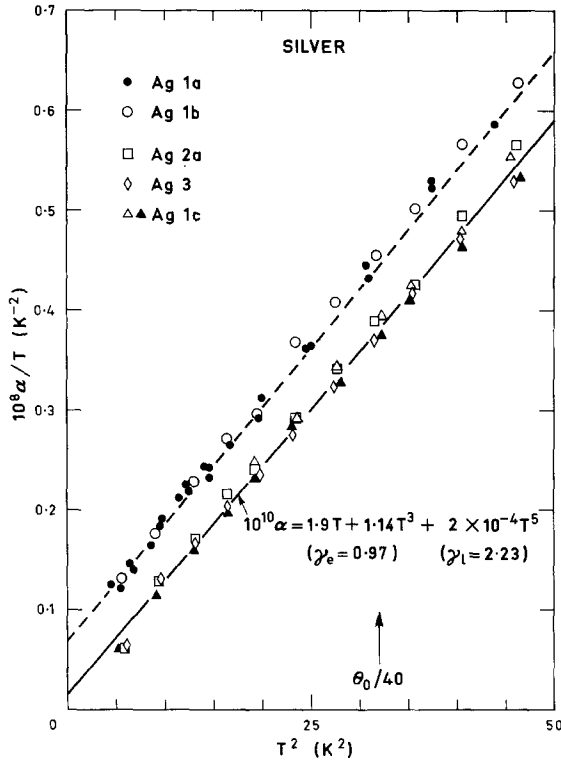


Fig. 8. Values of α/T vs. T^2 for silver ($\theta_0 = 226$ K) with computer-fitted polynomial; Ag 2, Ag 3, and Ag 1c are "oxygen-free."

from which we calculate

$$\gamma_e \approx 0.97 \pm 0.1 \quad \gamma_l = \gamma_0 \approx 2.23 \mp 0.06$$

Smoothed values for α , α_l , and γ_l are listed in Table V, and the temperature variation of γ_l is illustrated in Fig. 11.

3.4. Gold

The results for Au 1 and Au 2 listed in Table IV agree with each other and with data sent to us by Swenson⁹ (cf. Fig. 9) within ca. 1%, except at the lowest temperatures where the uncertainty is greater than this. Neither Au 1 nor Au 2 were of very high purity ($\gt 99.98\%$) so that differences in Fe and Mn impurity levels could contribute to the observed differences in α at liquid helium temperatures (Fig. 10).

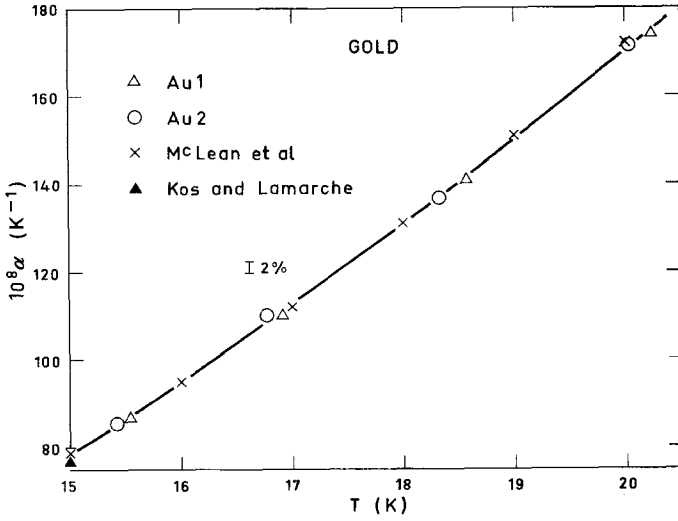


Fig. 9. Linear expansion coefficient of gold, 15–20 K.

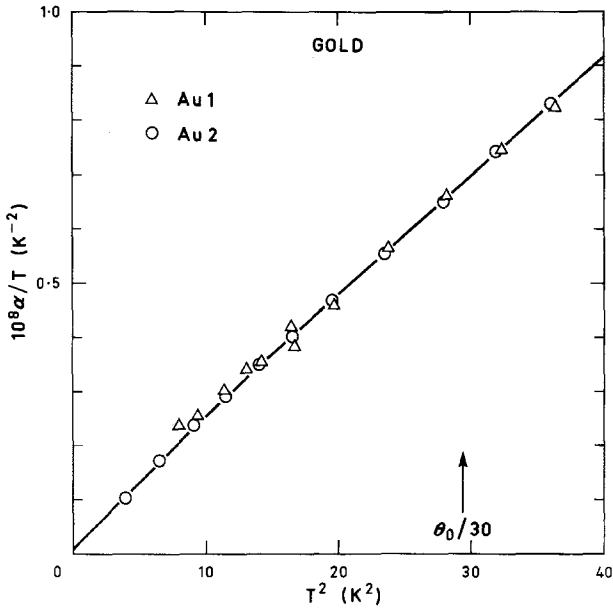


Fig. 10. α/T vs. T^2 for gold ($\theta = 162.5$ K). The curve represents the expression $10^{10}\alpha = 1T + 2.44T^3 - 0.005T^5$.

TABLE IV
 Linear Coefficient of Thermal Expansion α
 (Units of 10^{-8} K^{-1}) for Gold

Au 1		Au 2	
T	α	T	α
—	—	1.973	0.20
2.458	0.48 ₅	2.539	0.44
2.829	0.67	—	—
3.072	0.78	3.012	0.71 ₅
3.373	1.01	3.392	0.99
3.621	1.24	—	—
3.772	1.33	3.758	1.27
4.058	1.70	—	—
4.083	1.56	4.070	1.59
4.444	2.04	4.427	2.07
4.882	2.76	4.854	2.69
5.311	3.51	5.282	3.43
5.694	4.25	5.659	4.15
6.033	4.97	6.009	4.99
6.416	5.96	6.402	6.02
6.846	7.31	6.824	7.16
7.319	8.86	7.290	8.83
7.908	11.28	7.855	11.04
8.587	14.18	8.504	13.97
9.291	18.05	9.198	17.73
10.027	22.67	9.929	22.27
10.859	28.91	10.704	28.34
11.741	36.77	11.739	37.29
11.859	38.04	—	—
13.055	51.86	12.984	51.33
14.310	67.84	14.197	67.25
15.544	86.60	15.425	85.61
16.917	110.0	16.777	109.6
18.564	140.7	18.324	136.7
20.235	174.0	20.028	171.4
21.857	210.1	21.759	208.6
23.368	244.1	23.403	245.6
24.897	279.4	24.967	281.3
26.369	313.3	26.726	321.9
27.787	346.4	—	—
—	—	28.512	362.2
29.394	383.4	—	—

The expansion coefficient of Au does not fit well to a " $T + T^3$ " pattern over the temperature range of our measurements ($T > 2 \text{ K}$). It reflects the same type of variation as the specific heat for which $\theta(T)$ is still varying significantly below 1 K.^{32,33} Our measurements do not extend into the true Debye-continuum region for gold and we are unable to make an unequivocal

separation of the expansion coefficient into electronic and lattice components as we can with copper and silver.

Except for the two lowest experimental points from Au 1, which were of dubious accuracy, the data below 7 K can be fitted graphically (Fig. 10) by two straight lines:

$$10^{10}\alpha \simeq 1T + 2.45T^3 \quad T < 4 \text{ K}$$

$$10^{10}\alpha \simeq 4T + 2.2T^3 \quad 4 < T < 7 \text{ K}$$

In the region from 4 to 7 K, $\theta(T)$ goes through a broad maximum, remaining between 166 and 167 K^{32,33} ($\theta_0 = 162.5$ K). This is a good example of a pseudo- T^3 region in which quantitative interpretation of the separate T ("electronic") and T^3 ("lattice") terms is certainly erroneous.

Individual values of $\gamma(T)$ calculated for the experimental points below $\theta/10$ are about 2.94. We have therefore tried to fit a meaningful polynomial to the data by assuming $\gamma_0 = 2.94$ and $\gamma_e \simeq 0.7$ (i.e., the free-electron value), subtracting the corresponding values for the T^3 and T terms from the measured points and finding the T^5 term that gives the best fit. This is $-5.3 \times 10^{-13}T^5$. Note that the linear term is relatively so small that the analysis is insensitive to whether we choose $\gamma_e \simeq 0.7$ ($10^{10}\alpha_e \simeq 1.0T$) or $\gamma_e \simeq 0.9$ ($10^{10}\alpha_e \simeq 1.3T$). Below 7 K we may represent the expansion of gold by

$$10^{10}\alpha \simeq (1 \pm 0.5)T + (2.44 \mp 0.05)T^3 - (5 \pm 1) \times 10^{-3}T^5$$

In an alternative analysis we assumed $\gamma_l = \gamma_0 = 2.94$ below $\theta/10$ and calculated α_l using Eq. (5b). The remainder $(\alpha - \alpha_l)$ divided by T gave α_e as $\gtrsim 1T$ and $\gamma_l \gtrsim 0.7$, again with 50% uncertainty.

Smoothed values of the expansion coefficient at selected temperatures from 2 to 283 K are given in Table V.

4. DISCUSSION

4.1. The Lattice Grüneisen Parameter

The Grüneisen parameter is a measure of the anharmonicity of a solid. It can be calculated theoretically from specific models describing the volume and temperature dependence of contributions to the Helmholtz free energy from the ionic lattice, the electron gas, the spin system, etc., of a solid.⁷

The lattice parameter γ_l is generally calculated within the quasi-harmonic approximation in which the thermal free energy is a sum of independent contributions from the normal modes of vibration, assumed volume dependent [cf. Eqs. (2) and (3)]. At very low temperatures, $T \rightarrow 0$, only very

TABLE V

Mean Values of the Linear Expansion Coefficients α and Values for the Lattice Contributions, $\alpha_i = \alpha - \alpha_e$,^a and Lattice Grüneisen Parameter (Units of 10^{-8} K^{-1})

T	Copper			Silver			Gold		
	α	α_i	γ_l	α	α_i	γ_l	α	α_i	γ_l
2.0	0.06 ₆	0.02 ₃	1.79	0.13	0.09 ₁	2.24	0.21	0.19	2.93
2.5	0.09 ₈	0.04 ₄	1.79	0.23	0.18	2.25	0.40	0.38	2.94
3.0	0.14	0.077	1.79	0.37	0.31	2.24	0.68	0.65	2.95
3.5	0.20	0.12	1.80	0.56	0.49	2.25	1.05	1.02	2.96
4	0.27	0.18	1.80	0.81	0.73	2.24	1.55	1.51	2.98
5	0.46	0.36	1.80	1.53	1.43	2.25	2.94	2.89	2.97
6	0.75	0.62	1.79	2.59	2.48	2.25	4.94	4.88	2.93
7	1.13	0.98	1.79	4.08	3.94	2.25	7.8	7.73	2.94
8	1.64	1.47	1.80	6.1	5.90	2.23	11.6	11.52	2.94
9	2.29	2.10	1.79	8.7	8.53	2.21	16.6	16.51	2.94
10	3.10	2.89	1.79	12.0	11.81	2.21	22.8	22.7	2.93
12	5.30	5.04	1.77	21.5	21.3	2.22	40.1	39.98	2.93
14	8.65	8.35	1.80	36.0	35.7	2.24	64.2	64.1	2.94
15	10.70	10.37	1.79	44.8	44.5	2.23	78.5	78.3	2.93
16	13.10	12.75	1.79	55.5	55.2	2.24	95.0	94.8	2.94
18	19.2	18.8	1.79	80.5	80.1	2.24	131	130.8	2.94
20	27.1	26.7	1.79	111	110.6	2.24	171	170.8	2.94
22	37.2	36.7	1.78	147	146.6	2.24	214	213.8	2.94
24	49.4	48.9	1.77	187	186.5	2.25	259	258.8	2.94
25	56.4	55.6	1.77	209	208.5	2.26	283	282.8	2.95
26	64.0	63.5	1.77	231	230.5	2.26	305	304.7	2.94
28	81.5	80.9	1.79	278	277.4	2.26	351	350.7	2.94
30	101	100.4	1.81	326	325.4	2.26	397	396.7	2.95
32	123	122.4	1.81	378	377.4	2.28	—	—	—
34	148	147.3	1.83	—	—	—	—	—	—
57.5	509		1.90 ₅	966		2.35	875		2.96
65	626		1.92	1093		2.35	958		2.97 ₅
75	769		1.93 ₅	1229		2.37	1041		2.98
85	894		1.94 ₅	1338		2.38	1103		2.97 ₅
283	1643		1.98 ₅	1880		2.39	1408		2.96

^aUsing $10^8 \alpha_e/T = 0.021_5$ (Cu), 0.019 (Ag), and 0.010 (Au).

low frequency acoustic modes are excited in the lattice, which approximates an anisotropic continuum, and the limiting formula for $\gamma_l = \gamma_0$ is³⁴⁻³⁷

$$\gamma_0^{el} = \sum_i \int \gamma_i(\Omega) c_i^{-3/2}(\Omega) d\Omega / \sum_i \int c_i^{-3/2}(\Omega) d\Omega \quad (7)$$

$$\gamma_i(\Omega) = -\frac{1}{6} + \frac{1}{2} \{ [B_T/c_i(\Omega)] [dc_i(\Omega)/dP] \}_{T=0} \quad (8)$$

Here, $c_i(\Omega)$ is the elastic modulus for an acoustic wave of polarization i ($i = L, T_1, \text{ or } T_2$) propagated in direction Ω , and the integration is over all

TABLE VI
Physical Data for the Noble Metals

	Cu	Ag	Au
V (ml) 283 K ²⁹	7.11	10.28	10.21
4 K	7.04	10.15	10.10
B_3 (10^{11} dyn·cm ⁻²) 283 K ^{30,31}	13.75	10.39	17.34
4 K ^{30,31}	14.20	10.87	18.03
C_e/T (10^4 erg/mole K) ³²	0.695	0.650	0.729 ^a
θ_0 , K ³²	344.5	226	162.5

^aSubsequent to the N.B.S. compilation,³² Martin³³ has reported 0.691 for pure gold.

directions in the crystal, i.e., 4π steradians. References 34–37 describe various methods of performing the angular integration. The value so obtained for γ_0^{el} should agree with γ_0 within the combined experimental accuracy of the thermal measurements and the elastic measurements from which the pressure dependence of the moduli c_i is derived.

A number of people have measured the variation of the elastic moduli of the noble metals (Table VI) with either hydrostatic pressure or uniaxial stress. The latter measurements give values of the third-order elastic (TOE) moduli from which pressure derivatives can be calculated. Agreement between different estimates of γ_0^{el} is not good (Table VII), and some discussion is needed.

TABLE VII
Comparison of Thermal Grüneisen Parameters γ_0 and Elastic Values γ_0^{el} Calculated from Various Sets of Measurements of dc/dP and TOE Moduli Taken at the Temperatures Indicated^a

Data		Cu	Ag	Au
Thermal			γ_0	
White and Collins	($T \rightarrow 0$)	1.78	2.23	2.94
McLean <i>et al.</i> ⁹	($T \rightarrow 0$)	1.67	2.29	2.96
Elastic			γ_0^{el}	
Daniels and Smith ³⁸	(RT)	1.73	2.14	2.92
Ho <i>et al.</i> ³⁹	(RT)		2.16	
	($RT, 77$ K) ^b		2.12	
Salama and Alers ⁴⁰	(RT) ^c	1.64		
	(RT) ^d	1.65		
	(4.2 K) ^d	1.98		
Hiki and Granato ⁴¹	(RT) ^c	1.60	2.65	2.47
	(RT) ^d	1.79	2.49	2.45

^aValues of B_T and c_i used in Eq. (6) were for 4.2 K.^{30,31}

^bExtrapolated to $T = 0$ by volume from measurements between RT and 77 K.

^cCalculated from dc/dP given in the paper.

^dCalculated from dc/dP obtained from TOE moduli given in the paper.

The hydrostatic derivatives have not been measured at 4.2 K, i.e., effectively at $T = 0$, so either higher temperature results must be used in Eq. (8) or an extrapolation made using any available information on the temperature dependence of dc/dP or of the TOE moduli. The extrapolation cannot be made unambiguously because the information is conflicting. Measurements of the TOE moduli of copper⁴⁰ indicate that dc/dP increases by up to 20% for all three independent moduli as T falls from room temperature to zero, whereas measurements on silver³⁹ indicate slight decreases in two derivatives and a slight increase in the third. It is most unlikely that copper and silver behave in a qualitatively different way, and we infer that the experimental uncertainty in these difficult stress measurements at very low temperatures is probably comparable in magnitude with the apparent changes in the moduli and does not yet permit accurate extrapolation of room-temperature measurements to $T = 0$. It should be emphasized that hydrostatic measurements are much more reliable than uniaxial,^{40,42}

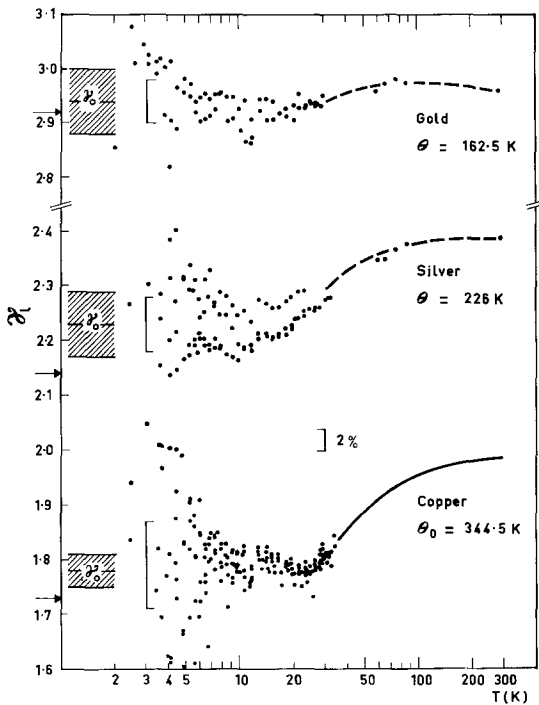


Fig. 11. Variation of the lattice Grüneisen parameter γ_l with temperature. Arrows show the best estimates of γ_l^0 , and the error bars at 3 K represent $\Delta\alpha \sim \pm 10^{-10} \text{ K}^{-1}$ (cf. Section 2.7).

and differences between them are evident in Table VII where one group of values of γ_0^{el} calculated directly from dc/dP differs from those calculated from TOE moduli obtained from the same experimental investigation.⁴¹

We consider that dc/dP may be assumed temperature independent within the accuracy of present elastic measurements, and choose the values obtained from the data of Daniels and Smith³⁸ as the best available estimates of γ_0^{el} for the noble metals. Correction of the measured isothermal-adiabatic derivatives to isothermal-isothermal derivatives required by theory⁴³ applies only to the modulus c_{11} and has a negligible effect on the final value of γ_0^{el} ($\Delta\gamma_0^{el} \sim 0.002$).

We have not compared thermal and elastic values of γ_l above the low-temperature limit. Barron⁸ has shown quite generally that γ_l changes most rapidly from its low- to its high-temperature limiting value in the region $\theta/20$ – $\theta/5$, and this is what is observed in practice. The rise in γ_l is just becoming evident in our measurements near 30 K (Fig. 11).

4.2. Electronic Grüneisen Parameter

The volume coefficient of expansion β_e of the electron gas in a metal is related to the electronic specific heat C_e by a Grüneisen relation (cf. Ref. 7)

$$\gamma_e = \beta_e B_T V / C_e$$

γ_e is also equal to the volume derivative of the electronic density of states per unit volume $N(\epsilon_F)$ at the Fermi surface

$$\gamma_e = 1 + (d \ln N(\epsilon_F) / d \ln V)_T$$

and can be estimated independently of the expansion measurements from knowledge of the change in the band structure of the metal with pressure. For free electrons with a spherical Fermi surface, increased pressure increases the volume within the Fermi surface required to contain one electron/atom without change of shape; the density of states is proportional to $V^{-1/3}$ and $\gamma_e = \frac{2}{3}$. For a real metal the energy surfaces are changed both in volume and in shape,^{44,45} and γ_e is no longer $\frac{2}{3}$.

The only theoretical estimates of γ_e for the noble metals have been made by Collins⁴⁶ for Cu, Ag, and Au, and by Davis *et al.*⁴⁷ for Cu alone; the values are listed in Table VIII along with those derived from our measurements of the electronic thermal expansion and those of McLean *et al.*⁹ Collins's estimate was based on a simple "cone model" of the Brillouin zone in which changes in shape under pressure of the (111) necks of the Fermi surface⁴⁴ were reproduced by allowing appropriate variations in the band-gap energies across the (111)-zone face. Collins's assumption that there is

TABLE VIII
Comparison of the Measured and Calculated Values of the
Electronic Grüneisen Parameter γ_e

	Cu	Ag	Au
Experimental			
White and Collins	0.93	0.97	≥ 0.7
McLean <i>et al.</i> ⁹	0.91	1.18	1.6
Theoretical			
Collins ⁴⁶	1.01	0.94	1.23
Davis <i>et al.</i> ⁴⁷	0.43		
free-electron model	0.67	0.67	0.67

negligible change in shape of the (001)-belly cross section is supported by later measurements.⁴⁵ Agreement with the experimental values of γ_e in Table VIII is quite good considering the simplicity of the model.

The estimate for copper by Davis *et al.*⁴⁷ is based on *a priori* band structure calculations for three different lattice spacings using the KKR method. It is smaller than the free-electron value in contrast to the experimental value which is larger. The reason for this is not obvious but may be related to their underestimation of the pressure dependence of the (111)-neck cross section, a region of the Fermi surface where the density of electron states is high and changing rapidly with neck size.

It has been suggested that “phonon enhancement” of the mass of a conduction electron might contribute to the electronic thermal expansion via its volume-dependent contribution to the free energy.⁴⁸ The present comparison with theoretical estimates throws no light on this question because the theoretical models are based on fits to observed properties, e.g., de Haas–van Alphen frequencies, of “enhanced” or “renormalized” electrons which already contain any such effect implicitly.

4.3. Summary

The foregoing discussion of our results in comparison with those of McLean *et al.*,⁹ and with theoretical estimates based on elastic measurements, has been on the basis of derived Grüneisen parameters γ_l and γ_e . The apparent differences in experimental values of γ (Tables VII and VIII) arise primarily from different methods of analysis, and *should not be allowed to obscure the remarkably good agreement found for the expansion coefficients over the whole temperature range in these two independent investigations.*

Measurements of the linear coefficient α are given for copper, silver,

and gold from 2–30, 57–85, and at 283 K. For Ag and Au values from 2–26 K agree with those in the accompanying paper⁹ to within 1 or 2%. In copper agreement is close from 18–30 K, but below this departures of 3–4% occur, our values lying between those reported by McLean *et al.* for Cu 1 and Cu 3. We conclude that, except possibly for Cu below 18 K, Table VI gives representative values which can be used as reference data with probable inaccuracies of less than 2%.

Gold has a low Debye temperature ($\theta_0 = 162.5$ K), and it is evident both from specific heat measurements³³ and from our inability to analyze the expansion data unambiguously into electronic and lattice components that the true Debye region does not commence until $T < 1$ K. At these temperatures the thermal expansion is so small ($< 10^{-10}$ K⁻¹) that present experimental methods are unlikely to give unequivocal results for the volume expansion of the conduction electrons and hence an accurate low-temperature polynomial expansion for α_e .

Elastic values for γ_0 based on room-temperature pressure derivatives agree satisfactorily with the present measurements; it is likely that measurements of dc/dP at liquid-helium temperatures or even near 60 K would give improved agreement with the thermal values.

ACKNOWLEDGMENTS

We thank Messrs A. van der Hoorn, C. Andrikidis, and K. Jensma who helped, respectively, with making the cryostat, preparing specimens, and taking data, and also Prof. C. A. Swenson with whom we have had many useful discussions and voluminous correspondence over the years.

REFERENCES

1. R. H. Carr, R. D. McCammon, and G. K. White, *Proc. Roy. Soc. (London)* **A280**, 72 (1964).
2. R. H. Carr and C. A. Swenson, *Cryogenics* **4**, 76 (1964).
3. J. M. Shapiro, D. R. Taylor, and G. M. Graham, *Can. J. Phys.* **42**, 835 (1964).
4. J. F. Kos and J. L. G. Lamarche, *Can. J. Phys.* **47**, 2509 (1969).
5. F. N. D. Pereira, C. H. Barnes, and G. M. Graham, *J. Appl. Phys.* **41**, 5050 (1970).
6. G. M. Graham, Univ. of Toronto, to be published.
7. J. G. Collins and G. K. White, *Progr. Low Temp. Phys.* **4**, 450 (1964).
8. T. H. K. Barron, *Phil. Mag.* **46**, 720 (1955).
9. K. O. McLean, C. A. Swenson, and C. R. Case, *J. Low Temp. Phys.* **7**, 77 (1972) (the following paper in this issue).
10. G. K. White, *Cryogenics* **1**, 151 (1961).
11. J. S. Rogers, R. J. Tainsh, M. S. Anderson, and C. A. Swenson, *Metrologia* **4**, 47 (1968).
12. C. P. Pickup and W. R. G. Kemp, *Cryogenics* **9**, 90 (1969).
13. R. H. Carr, R. D. McCammon, and G. K. White, *Phil. Mag.* **12**, 157 (1965).
14. P. W. Sparks and C. A. Swenson, *Phys. Rev.* **163**, 779 (1967).
15. H. Ibach, *Phys. Status Solidi* **31**, 625 (1969).
16. G. K. White, *Proc. Roy. Soc. (London)* **A286**, 204 (1965).

17. G. K. White and A. T. Pawlowicz, *J. Low Temp. Phys.* **2**, 631 (1970).
18. G. K. White, *Proc. First Thermal Expansion Symp.*, Washington, 1968, to be published.
19. G. K. White, to be published.
20. T. Rubin, H. W. Altman, and H. L. Johnston, *J. Am. Chem. Soc.* **76**, 5289 (1954).
21. T. A. Hahn, *J. Appl. Phys.* **41**, 5096 (1970); C. G. Kirby and H. Preston-Thomas, private communication, 1968.
22. G. Hetherington and K. H. Jack, *Phys. Chem. Glasses* **3**, 129 (1962).
23. D. N. Batchelder and R. O. Simmons, *J. Chem. Phys.* **41**, 2324 (1964).
24. D. F. Gibbons, *Phys. Rev.* **112**, 136 (1958).
25. G. K. White, *Proc. Third Symp. on Thermal Expansion*, Corning, N.Y., 1971.
26. R. K. Kirby and T. A. Hahn, private communication, 1970.
27. T. H. K. Barron and J. A. Morrison, *Can. J. Phys.* **35**, 799 (1957).
28. M. Blackman, *Handb. d. Phys.* **VII/1**, 325 (1955).
29. *American Institute of Physics Handbook*, 2nd ed. (McGraw-Hill, New York, 1963).
30. W. C. Overton and J. Gaffney, *Phys. Rev.* **98**, 969 (1955).
31. J. R. Neighbours and G. A. Alers, *Phys. Rev.* **111**, 707 (1958).
32. G. T. Furukawa, W. G. Saba, and M. L. Reilly, NSRDS-NBS 18, U.S. Govt. Printing Office, Washington, D.C., 1968.
33. D. L. Martin, *Phys. Rev.* **170**, 650 (1968).
34. F. W. Sheard, *Phil. Mag.* **3**, 1381 (1958).
35. W. B. Daniels, *Phys. Rev. Letters* **8**, 3 (1962).
36. J. G. Collins, *Phil. Mag.* **8**, 323 (1963).
37. D. E. Schuele and C. S. Smith, *J. Phys. Chem. Solids* **25**, 801 (1964).
38. W. B. Daniels and C. S. Smith, *Phys. Rev.* **111**, 713 (1958).
39. P. S. Ho, J. P. Poirier, and A. L. Ruoff, *Phys. Status Solidi* **35**, 1017 (1969).
40. K. Salama and G. A. Alers, *Phys. Rev.* **161**, 673 (1967).
41. Y. Hiki and A. V. Granato, *Phys. Rev.* **144**, 411 (1966); see also Y. Hiki, A. V. Granato, and J. F. Thomas, *Phys. Rev.* **153**, 764 (1967).
42. C. S. Smith, private communication.
43. G. R. Barsch and Z. P. Chang, *Phys. Status Solidi* **19**, 139 (1967).
44. I. M. Templeton, *Proc. Roy. Soc. (London)* **A292**, 413 (1966).
45. W. J. O'Sullivan and J. E. Schirber, *Phys. Rev.* **170**, 667 (1968).
46. J. G. Collins, *Ann. Acad. Sci. Fennicae* **AVI**, No. 210, 239 (1966).
47. H. L. Davis, J. S. Faulkner, and H. W. Joy, *Phys. Rev.* **167**, 601 (1968).
48. R. W. Munn, *Phys. Letters* **29A**, 395 (1969).